



Article

Antioxidant and Cytoprotective Properties of Polyphenol-Rich Extracts from *Antirhea borbonica* and *Doratoxylon apetalum* against Atherogenic Lipids in Human Endothelial Cells

Jonathan Bonneville ^{1,2}, Philippe Rondeau ², Bryan Veeren ², Julien Faccini ^{1,3}, Marie-Paule Gonthier ², Olivier Meilhac ^{2,4,*} and Cécile Vindis ^{1,3,*}

¹ Clinical Investigation Center (CIC) 1436, INSERM 1048, 31400 Toulouse, France; jon.bonneville@gmail.com (J.B.); cecile.vindis1@inserm.fr (J.F.)

² Université de la Réunion, 97400 La Réunion, France; rophil@univ-reunion.fr (P.R.); bryan.veeren@univ-reunion.fr (B.V.); marie-paule.gonthier@univ-reunion.fr (M.-P.G.)

³ Université de Toulouse III Paul Sabatier, 31400 Toulouse, France

⁴ CHU de La Réunion, Saint-Pierre, 97448 La Réunion, France

* Correspondence: olivier.meilhac@inserm.fr (O.M.); cecile.vindis@inserm.fr (C.V.)

Citation: Bonneville, J.; Rondeau, P.; Veeren, B.; Faccini, J.; Gonthier, M.-P.; Meilhac, O.; Vindis, C. Antioxidant and Cytoprotective Properties of Polyphenol-Rich Extracts from *Antirhea borbonica* and *Doratoxylon apetalum* against Atherogenic Lipids in Human Endothelial Cells. *Antioxidants* **2022**, *11*, 34. <https://doi.org/10.3390/antiox11010034>

Academic Editor: Wei Chen

Received: 29 November 2021

Accepted: 22 December 2021

Published: 24 December 2021

Publisher's Note: MDPI stays neutral with regard to jurisdictional claims in published maps and institutional affiliations.



Copyright: © 2021 by the authors. Licensee MDPI, Basel, Switzerland. This article is an open access article distributed under the terms and conditions of the Creative Commons Attribution (CC BY) license (<https://creativecommons.org/licenses/by/4.0/>).

Abstract: The endothelial integrity is the cornerstone of the atherogenic process. Low-density lipoprotein (LDL) oxidation occurring within atheromatous plaques lead to deleterious vascular effects including endothelial cell cytotoxicity. The aim of this study was to evaluate the vascular antioxidant and cytoprotective effects of polyphenol-rich extracts from two medicinal plants from the Reunion Island: *Antirhea borbonica* (*A. borbonica*), *Doratoxylon apetalum* (*D. apetalum*). The polyphenol-rich extracts were obtained after dissolving each dry plant powder in an aqueous acetonetic solution. Quantification of polyphenol content was achieved by the Folin–Ciocalteu assay and total phenol content was expressed as g gallic acid equivalent/100 g plant powder (GAE). Human vascular endothelial cells were incubated with increasing concentrations of polyphenols (1–50 μ M GAE) before stimulation with oxidized low-density lipoproteins (oxLDLs). LDL oxidation was assessed by quantification of hydroperoxides and thiobarbituric acid reactive substances (TBARS). Intracellular oxidative stress and antioxidant activity (catalase and superoxide dismutase) were measured after stimulation with oxLDLs. Cell viability and apoptosis were quantified using different assays (MTT, Annexin V staining, cytochrome C release, caspase 3 activation and TUNEL test). *A. borbonica* and *D. apetalum* displayed high levels of polyphenols and limited LDL oxidation as well as oxLDL-induced intracellular oxidative stress in endothelial cells. Polyphenol extracts of *A. borbonica* and *D. apetalum* exerted a protective effect against oxLDL-induced cell apoptosis in a dose-dependent manner (10, 25, and 50 μ M GAE) similar to that observed for curcumin, used as positive control. All together, these results showed significant antioxidant and antiapoptotic properties for two plants of the Reunion Island pharmacopeia, *A. borbonica* and *D. apetalum*, suggesting their therapeutic potential to prevent cardiovascular diseases by limiting LDL oxidation and protecting the endothelium.

Keywords: *Antirhea borbonica*; *Doratoxylon apetalum*; polyphenol; oxidized LDL; vascular cell

1. Introduction

Among the different risk factors of cardiovascular disease, high levels of low-density lipoprotein cholesterol (LDL-C) remain the major determinant of lipid accumulation within the arterial wall and subsequent atherosclerotic plaque formation. LDL oxidation is responsible for their unregulated uptake by phagocytes, thereby forming foam cells [1]. In the subendothelial space of large arteries, LDL undergo oxidation via different mechanisms involving reactive oxygen species produced by vascular cells and leukocytes in the

presence of transition metals such as iron contained in hemin [2]. In the first steps of atherogenesis, oxidized LDLs (oxLDLs) induce the expression of adhesion molecules such as VCAM-1 and ICAM-1 (respectively vascular and intercellular cell adhesion molecules) that promote leukocyte infiltration [3]. Lipids contained in oxLDLs stimulate the expression of pro-angiogenic factors such as vascular endothelial growth factor A by smooth muscle cells, which promotes angiogenesis even in the early stages of atherogenesis [4]. Neoangiogenesis favors intraplaque growth and subsequent hemorrhage that participate in further cholesterol accumulation and erythrocyte extravasation. OxLDLs also display deleterious cytotoxic effects for leukocytes and for different vascular cells, including endothelial cells [5,6]. Disruption of the endothelial layer leads to increased leukocyte extravasation and represents a key factor in destabilizing the plaque towards rupture and ultimately clinical complications.

Different strategies may be used to limit both LDL oxidation and their deleterious effects [7]. Although antioxidant-based dietary interventions may exert a protective effect on cardiovascular disease, supplementation by specific antioxidants such as vitamins E and C, was disappointing [8]. Nutritional approaches that rely on the use of medicinal plants may help to reduce oxidative stress, particularly by counteracting lipid oxidation. Polyphenols are the most abundant antioxidants contained in plant-based beverages [9]. For example, curcumin was long known to inhibit LDL oxidation and the proatherogenic effects of oxLDLs both in vitro and in vivo [10].

Antirhea borbonica (*A. borbonica*) and *Doratoxylon apetalum* (*D. apetalum*) are two medicinal plants from Reunion Island traditionally used for their astringency, hemostatic or anti-inflammatory properties. *A. borbonica* is referenced in the French Pharmacopeia, among 27 other medicinal plants from Reunion Island. The choice of these 2 plants relies on their high content in total polyphenols such as phenolic acids and flavonoids, in particular for *D. apetalum* [11]. We showed that the polyphenols contained in these plants have anti-inflammatory and antioxidant effects on adipose cells exposed to different types of bacterial lipopolysaccharides (LPS) [11,12].

In this study, we hypothesized that polyphenol-rich extracts from *A. borbonica* and *D. apetalum* may reduce LDL oxidation and oxidative stress-induced cytotoxicity of oxLDLs on human vascular endothelial cells.

2. Materials and Methods

2.1. Reagents

Curcumin, 2-thiobarbituric acid (TBA), malondialdehyde (MDA) and 4',6'-diamino-2-phenylidone (DAPI) were from Sigma-Aldrich (St Louis, USA). 3-(4,5-dimethylthiazol-2-yl)-2,5-diphenyltetrazolium bromide (MTT) were from Euromedex (Souffelweyersheim, France). SYTO-13, propidium iodide (PI), 6-carboxy-2',7'-dichlorodihydrofluorescein diacetate (H₂DCFDA) were from Molecular Probes (Invitrogen, San Diego, CA). Cleaved Caspase-3 antibody was from Abcam (Paris, France) and secondary antibody was from Life technologies (Thermo Fisher Scientific, Carlsbad, CA).

2.2. Extraction and Quantification of Polyphenols in Medicinal Plant Extracts

A. borbonica and *D. apetalum* medicinal plants were collected in Réunion Island and botanically identified with voucher numbers (Table 1). After airflow drying (45 °C), plant organs were reduced to powder. Polyphenol-rich extracts from medicinal plants were obtained after dissolving each plant powder (2 g) in 20 mL of an aqueous acetonetic solution (70%, v/v) as described previously [11]. A calibration curve was prepared using a standard solution of gallic acid (Sigma–Aldrich, Taufkirchen Germany). The total phenol content was expressed as mg gallic acid equivalent (GAE)/g plant powder.

Table 1. Global description of medicinal plants tested.

Botanical Name	Family	Voucher Number	Parts Used
<i>Doratoxylon apetalum</i> ^a (Poir.) Radlk	Sapindaceae	RUN-055E	Leaf
<i>Antirhea borbonica</i> ^b J.F Gmelin	Rubiaceae	RUN-052F	Leaf, stem

Common names: ^a: Bois de gaulette; ^b: Bois d'Osto.

2.3. Polyphenol Compound Identification by UPLC-UV-ESI-MS/MS

Identification of polyphenols of *A. borbonica* and *D. apetalum* plant extracts was carried out by ultra-high-performance liquid chromatography (UHPLC) coupled with diode array detection and a HESI-Orbitrap mass spectrometer (Q Exactive Plus, Thermo Fisher), according to the method previously used by Delveaux et al., with slight modifications [13].

2.4. LDL Isolation and Oxidation

Plasma was obtained from healthy volunteers within the framework of an agreement between INSERM and the French Blood Establishment, in accordance with the provisions of Article L.1243-3 of the Public Health Code, which provides for its use for research purposes. LDL were isolated by ultracentrifugation from a pool of human plasma and mildly oxidized by UV-C in the presence of 5 μM CuSO_4 as we previously reported [14]. Oxidized LDLs contained 4.2 to 7.4 nmoles of thiobarbituric acid-reactive substances (TBARS)/ μg apoB measured according to Yagi et al. [15]. Relative electrophoretic mobility (REM) and 2,4,6-trinitrobenzenesulfonic acid (TNBS) reactive amino groups were 1.2–1.3 times and 85–92% of native LDL, respectively.

2.5. Lipid Hydroperoxide Assay

Conjugated diene at 234 nm could not be quantified due to interference of the plant extracts at this wavelength. Lipid hydroperoxides were measured by a modified version of the Ferrous ion Oxidation of Xylenol orange (FOX) assay [16,17]. Briefly, 200 μg apoB/mL of LDL were incubated for 2 h at 37 °C in 500 μL PBS containing 4 μM CuSO_4 with or without polyphenol-rich extracts. 50 μL of this solution were then added to 450 μL of a solution containing 1 part of solution A (250 mM of sulfuric acid, 2.5 mM of ferrous sulfate and 1 mM xylenol orange) to 9 parts of solution B (4.4 mM of butylated hydroxytoluene in 100% methanol). After 30 min incubation at room temperature (RT) protected from light, the samples were vortex-mixed and then centrifuged for 10 min at 12,000 g. The optical density of the supernatant was then measured at 560 nm.

2.6. Cell Culture

Human microvascular endothelial cells (HMEC-1) were from ATTC. HMEC-1 cell line is an immortalized human dermal microvascular endothelial cell line expressing von Willebrand's factor (vWF), cell adhesion molecules such as ICAM-1, and are capable of oxidized LDLs uptake. Cells were grown in MCDB-131 culture medium as we previously described [18]. The cells were starved in serum-free medium 24 h before the experiments.

2.7. THIOBARBITURIC Acid-Reactive Substances Assay

TBARS levels were assessed by the thiobarbituric acid reaction as previously described [15]. TBARS levels were detected in cell culture medium after 6 h of cell exposure to 50 μg apoB/mL native LDL and 1.5 μM CuSO_4 , in the presence or not of various concentrations of polyphenol-rich extracts. Briefly, 100 μL of cell culture medium were added to 100 μL of a 0.375% TBA/15% trichloroacetic acid in 0.25 N HCl, incubated for 10 min at 95 °C, and clarified by centrifugation (400 g for 10 min). The fluorescence was quantified

in the supernatant using a TECAN fluorescent spectrophotometer (excitation at 515 nm, emission at 548 nm) by comparison with a standard curve of MDA. TBARS levels were expressed as μM of MDA.

2.8. Quantification of Intracellular Reactive Oxygen Species

The generation of intracellular reactive oxygen species (ROS) in endothelial cells was performed as previously described [19] using the 6-carboxy-2',7'-dichlorodihydrofluorescein diacetate (H₂DCFDA) ROS-sensitive fluorescent probe (5 μM). Briefly, cells grown in 12-well plates until confluence were incubated with the probe for 30 min at 37 °C, and then stimulated with oxLDLs in the presence or not of each plant extract for 1 h before analysis. The data are expressed as ratio of fluorescence/fluorescence of the nonstimulated control.

2.9. Evaluation of Cytotoxicity, Necrosis and Apoptosis

2.9.1. Cell Viability Test

Cytotoxicity was evaluated using the MTT [3-(4,5-dimethylthiazol-2-yl)-2,5-diphenyltetrazolium bromide] test, as we previously described [14]. After cell treatment, MTT (5 mg/mL) were added to each well at a final concentration of 0.5 mg/mL, followed by 4 h of incubation at 37 °C. A solution of dimethylsulfoxide was added to each well to dissolve formazan crystals and absorbance was read at 595 nm. Results are expressed as the percentage of untreated cells.

2.9.2. Apoptotic Versus Necrotic Cell Count by Fluorescence Microscopy

Apoptotic and necrotic cells were counted after staining by two fluorescent dyes, the permeant DNA intercalating green probe SYTO-13 (0.6 μM) and the nonpermeant DNA intercalating red probe propidium iodide (15 μM) using an inverted fluorescence microscope (Fluovert FU, Leitz) [14]. Normal nuclei exhibit a loose, green-colored chromatin whereas primary necrotic cells exhibit loose red-colored chromatin. Apoptotic nuclei showed a condensed yellow/green-colored chromatin associated with nucleus fragmentation, and postapoptotic necrotic cells presented the same morphological features but were red-colored.

2.9.3. Determination of Phosphatidylserine Exposure by Flow Cytometry

Annexin-V-FITC labeling were performed to evaluate phosphatidylserine externalization, an early event of apoptosis. Annexin V staining of HMEC-1 cells was evaluated by flow cytometry using a CytoFLEX (Beckman Coulter) and CytExpert software. Cells were detached with trypsin, washed with PBS and then labeled with 2 $\mu\text{g}/\text{mL}$ Annexin V-FITC (dilution in binding buffer, BioLegend) for 15 min at RT. Targeted cell population selected by gating was identified by its typical location in a FSC vs. SSC graph.

2.9.4. In Situ Detection of Cytochrome C

HMEC-1 cells grown on glass coverslips were fixed in PBS-4% paraformaldehyde (PFA) for 10 min at RT, washed and permeabilized with 0.1% TritonX100 for 10 min at RT. After blocking of the non-specific sites with PBS containing 3% bovine serum albumin (BSA), cells were incubated with an anti-cytochrome C primary antibody (1:100 dilution, mouse mAb,12963, Cell Signaling Technology, Saint Quentin Yvelines, France) for 1 h at RT and revealed with Alexa Fluor-conjugated secondary antibody (1:1000 dilution). Cell nuclei were stained with 4',6-diamidino-2-phenylindole (DAPI) and images were acquired on a Zeiss LSM 780 confocal microscope.

2.9.5. In Situ Detection of Caspase 3 Activation

HMEC-1 cells grown on glass coverslips were fixed in PBS-4% PFA for 10 min at RT. After blocking of the nonspecific sites with PBS containing 2% BSA for 30 min, cells were

incubated with a polyclonal anticlaved caspase-3 antibody (1:100 dilution, Abcam, ab13847) for 1 h at RT and revealed with Alexa Fluor-conjugated secondary antibody (1:200 dilution). Cell nuclei were stained with DAPI and images were captured with an Eclipse 80i Nikon fluorescence microscope equipped with a Hamamatsu ORCA-ER digital camera (Life Sciences, Japan). For quantification, 3 representative fields were used for each condition and the fluorescence intensity of images was analyzed with ImageJ software (<http://rsb.info.nih.gov/ij/>, version 1.32j, accessed on 23 November 2021).

2.9.6. In Situ Cell Apoptosis Detection by TUNEL

Terminal transferase dUTP nick-end (TUNEL) technique was used for the detection of fragmented DNA (in situ Cell Death Detection Kit- Roche). HMEC-1 cells were fixed in PBS-4% PFA for 10 min at RT and processed following the manufacturer's protocol. Cell nuclei were counterstained with DAPI and images were captured with an Eclipse 80i Nikon fluorescence microscope equipped with a Hamamatsu ORCA-ER digital camera (Life Sciences, Japan). 3 representative fields were used for each condition for quantification of cell death. Results are expressed as a percentage of TUNEL-positive nuclei compared to the total number all nuclei (DAPI-labeled nuclei).

2.10. Determination of LDL Cellular Uptake

LDL uptake was measured by using native LDL labeled with the fluorescent lipid dye 3,3'-dioctadecyl-indocarbocyanine (DiI, 300 µg, Molecular Probes), as we previously described [20]. The DiI content was measured by a TECAN fluorescent spectrophotometer (excitation 520 nm, emission 568 nm). Values are expressed as fold of control after normalization to total protein content.

2.11. Cell Protein Extraction and Quantification

After treatment, total proteins were obtained from cell lysis by the freeze-thaw method consisting in 5 successive cycles of fast freezing in liquid nitrogen and subsequent thawing in 37 °C water bath. Protein concentration was quantified by the bicinchoninic acid assay (BCA, Sigma).

2.12. Catalase and Superoxide Dismutase Activity Assays

The catalase activity assay was carried out on 30 µg of protein lysate. Blanks were measured at 240 nm just before adding 80 µL of H₂O₂ (10 mM final) to start the reaction. H₂O₂ reduction was monitored by measuring the absorbance every 5 s at 240 nm for 1 min. Catalase activity was calculated using a calibration standard curve with increasing amounts of catalase between 12.5 and 125 units/mL and expressed as international catalytic units per microgram of proteins.

The total superoxide dismutase (SOD) activity was quantified using the cytochrome C reduction assay. Superoxide radicals generated by the xanthine/xanthine oxidase system reduce the ferricytochrome C into ferrocyanochrome C, which then leads to an increase in absorbance at 560 nm. About 20 µg of cell lysate were combined with the reaction mixture (xanthine oxidase, xanthine (0.5 mM), cytochrome C (0.2 mM), KH₂PO₄ (50 mM) and EDTA (2 mM)). The reaction was monitored in a microplate reader at 560 nm for 1 min, the SOD activity was calculated using a calibration standard curve of SOD (0 to 6 units/mg) and expressed as international catalytic units per microgram of proteins.

2.13. Western Blot Analysis

For western blot analysis, total proteins were extracted in a solubilization buffer as described [14], resolved by SDS-polyacrylamide gel electrophoresis and transferred onto polyvinylidene fluoride (PVDF) membranes (Immobilon, IPVH 00010, Merck Millipore, Molsheim, France). Membranes were probed with caspase 3 antibody (1:1000, rabbit, 9662, Cell Signaling Technology, Saint Quentin Yvelines, France) and revealed with secondary

antibodies coupled to horseradish peroxidase (ECL chemoluminescence kit, Amersham, Pittsburgh, PA, USA) using the Chemidoc Touch system (Bio-Rad, Marnes-la-Coquette, France). Stripped membranes were reprobated with an anti- β -actin antibody to control the equal loading of proteins. Quantification of protein bands was performed using Image Lab software (Image Lab 6.0.1, Bio-Rad, Marnes-la-Coquette, France).

2.14. Statistical Analysis

Results were expressed as means \pm SEM. Differences between two groups were analyzed by an unpaired two-tailed Student's *t*-test. Differences between more than two groups were analyzed by one-way analysis of variance (ANOVA) with Tukey's *posthoc* test for multiple comparisons. Statistical significance was set to $p < 0.05$.

3. Results

3.1. Polyphenol Content of *D. Apetalum* and *A. Borbonica* Plant Extracts

Dietary polyphenols represent the most abundant antioxidants provided by the human diet. Previous studies performed in our laboratory have led us to focus on 2 plants from Reunion Island widely used by the population for their anti-inflammatory properties, namely *D. apetalum* and *A. borbonica*. These 2 plants contain large amounts of polyphenols and were shown to reduce the production of interleukin-6 and MCP-1 in pre-adipocytes exposed to TNF- α , H₂O₂ or lipopolysaccharides [11]. The identification of polyphenols of acetonic extracts of *D. apetalum* and *A. borbonica*, was performed by mass spectroscopy. Figures S1 and S2 show the total ion chromatogram (TIC) and chromatographic profiles (recorded at 315 nm) of *D. apetalum* and *A. borbonica* extracts, respectively. For *D. apetalum*, a total of 17 main compounds, numbered according to their elution order, were identified and reported in Table 2 with their retention time, experimental *m/z* mass, corresponding chemical formulas and their main MS/MS fragments.

Table 2. Polyphenols identified in *D. apetalum* plant extract.

Peak Number	RT (min)	Compound	Molecular Formula	Mass Error (ppm)	[M-H] ⁻	MS/MS Fragments
1	2.1	Protocatechuic acid	C ₇ H ₆ O ₄	0	153.0182	109.0282
2	2.3	Gallic acid 4-O-glucoside	C ₁₃ H ₁₅ O ₁₀	2.4	331.0668	168.0053, 125.0231, 211.0238
3	2.7	Unknown	C ₁₅ H ₁₈ O ₈	2.6	325.0927	
4	3.1	Unknown	C ₁₃ H ₁₂ O ₈	2.5	295.0456	163.0389, 112.9867
5	3.3	Procyanidin dimer type B	C ₃₀ H ₂₆ O ₁₂	5.1	577.1371	289.0714, 407.0766, 125.0231, 109.0282
6	3.7	Epicatechin	C ₁₅ H ₁₅ O ₆	2.7	289.0715	245.0814, 179.0340, 125.0232, 109.0282
7	3.9	Procyanidin trimer type C	C ₄₅ H ₃₈ O ₁₈	1.2	865.1985	289.0714, 411.0718, 125.0232, 109.0283, 560.0907
8	4.4	Coumaric acid	C ₉ H ₈ O ₃	0	163.039	119.049
9	4.7	Quercetin 3-O-rutinoside (Rutin)	C ₂₇ H ₃₀ O ₁₆	1.7	609.1461	301.0348
10	4.7	Unknown	C ₁₃ H ₁₂ O ₇	2.7	279.0507	133.0130, 163.0390
11	4.9	Kaempferol 3-O-rutinoside	C ₂₇ H ₃₀ O ₁₉	1.3	593.1509	285.04
12	4.9	Quercetin 3-O-hexoside	C ₂₁ H ₁₉ O ₁₂	0.5	468.0881	301.0347
13	5.1	Kaempferol 3-O-hexoside	C ₂₁ H ₂₀ O ₁₁	2	447.0931	285.0402
14	5.5	Apigenin-7-O-rutinoside (Isorhoifolin)	C ₂₇ H ₃₀ O ₁₄	1.8	577.1563	269.0453

15	5.7	Apigenin hexoside	C ₂₁ H ₂₀ O ₁₀	1.6	431.0984	269.0453
16	5.9	Kaempferol 3-O-(6-malonyl-hexoside)	C ₂₄ H ₂₂ O ₁₄	1.5	533.0934	489.1035, 285.0401
17	6.5	Apigenin	C ₁₅ H ₁₀ O ₅	3.1	269.0454	

Polyphenol-rich *D. apetalum* extract was analyzed by using a Q Exactive Plus mass spectrometer. Compounds were identified according to their retention time (min)/molecular weight (Da) (see spectra on Figure S1).

The main polyphenols identified were three kaempferol derivatives (kaempferol 3-O-rutinoside, kaempferol 3-O-hexoside and kaempferol 3-O-(6-malonyl-hexoside)), two quercetin derivatives (quercetin 3-O-rutinoside (Rutin) and quercetin 3-O-hexoside) and two procyanidin derivatives (dimer type B and trimer type C). Several minority polyphenols were also identified such as apigenin or gallic acid 4-O-glucoside. For *A. borbonica*, a total of 21 main compounds were identified and reported in Table 3. The main polyphenols identified were several dicaffeoylquinic acids derivatives, caffeic acid, and quercetin derivatives. Coumaric acid, 5-feruloylquinic acid and protocatechuic acid are three polyphenols identified among the minority compounds.

Table 3. Polyphenols identified in *A. borbonica* plant extract.

Peak Number	RT (min)	Compound	Molecular Formula	Mass Error (ppm)	[M-H] ⁻	MS/MS Fragments
1	0.6	Quinic acid	C ₆ H ₁₂ O ₇	-0.3	195.0499	127.0388, 111.0438
2	2.1	Protocatechuic acid	C ₇ H ₆ O ₄	-0.2	153.018	109.0281
3	2.4	5-Caffeoylquinic acid	C ₁₆ H ₁₈ O ₁₀	0.23	353.0869	191.0549, 179.0337, 173.0442, 135.0437
4	2.6	hydroxybenzoic acid isomer	C ₇ H ₆ O ₃	-0.29	137.023	93.0331
5	3.3	5-Caffeoylquinic acid	C ₁₆ H ₁₈ O ₉	0.23	353.0869	191.0549, 179.0337, 173.0443, 135.0437
6	3.5	Caffeic acid	C ₉ H ₈ O ₄	-0.14	179.0337	135.0438
7	4	5-p-Coumaroylquinic acid	C ₁₆ H ₁₇ O ₈	0.2	337.092	191.0549, 173.0442, 93.0331
8	4.1	o/m-Coumaric acid	C ₁₅ H ₁₀ O ₄	-0.2	163.0387	119.0488
9	4.4	p-Coumaric acid	C ₁₅ H ₁₀ O ₄	-0.2	163.0387	119,30,488
10	4.4	5-Feruloylquinic acid	C ₁₇ H ₂₀ O ₉	0.2	367.1026	
11	4.8	Quercetin 3-O-rutinoside	C ₂₇ H ₃₀ O ₁₆	0.1	609.1448	301.0341
12	5	Quercetin 3-O-hexoside	C ₂₁ H ₂₀ O ₁₂	0.1	463.087	300.0268
13	5.1	Kaempferol 3-O-galactoside 7-O-rhamnoside	C ₂₇ H ₃₀ O ₁₅	0.1	593.15	284.032
14	5.5	3,5-Dicaffeoylquinic acid	C ₂₅ H ₂₄ O ₁₂	-0.2	515.1182	191.0550, 179.0338, 353.0870, 135.0438
15	6	Unknown	C ₂₆ H ₃₂ O ₁₄	-0.01	567.1719	163.0387, 195.0650, 315.1231, 359.1124, 521.1653
16	6	hydroxybenzoic acid isomer	C ₇ H ₆ O ₃	-0.29	137.023	93.0331
17	6.1	3,4-Dicaffeoylquinic acid	C ₂₅ H ₂₄ O ₁₂	-0.2	515.1182	353.0870, 173.0443, 191.0549, 135.0437
18	6.2	5-Caffeoylquinic acid	C ₁₆ H ₁₈ O ₁₁	0.05	353.0868	
19	6.5	1,4/4,5-Dicaffeoylquinic acid	C ₂₅ H ₂₄ O ₁₂	-0.1	515.1183	173.0443, 353.0869, 191.0549, 135.0436
20	7.3	Quercetin	C ₁₅ H ₁₀ O ₇	0.9	301.0345	
21	8.2	Kaempferol	C ₁₅ H ₁₀ O ₆	1.3	285.0405	

Polyphenol-rich *A. borbonica* extract was analyzed by using a Q Exactive Plus mass spectrometer. Compounds were identified according to their retention time (min)/molecular weight (Da) (see spectra on Figure S2).

Total polyphenol content of acetonic extracts obtained from these 2 medicinal plants was also evaluated by using Folin–Ciocalteu assay. As shown in Table 4, *D. apetalum* extract displays a higher polyphenol content (3.79 mg GAE/g plant) compared to *A. borbonica* extract (1.98 mg GAE/g plant). Description and identification of the different polyphenols contained in these plants was previously published by our group [11].

Table 4. Total polyphenol content of *D. apetalum* and *A. borbonica* plant extracts.

	Total Polyphenol Content (mg GAE/g plant)
<i>Doratoxylon apetalum</i>	3.79 ± 0.14
<i>Antirhea borbonica</i>	1.98 ± 0.09

Polyphenols levels were determined by a colorimetric assay and expressed as mg gallic acid equivalent (GAE)/g of dry plant powder. Data are means ± SEM of four independent experiments.

3.2. *A. Borbonica* and *D. Apetalum* Extracts Prevent the Oxidation of LDL

Since polyphenols are widely recognized antioxidants, we tested the ability of *D. apetalum* and *A. borbonica* extracts to inhibit copper-induced LDL oxidation by measuring the formation of hydroperoxides. LDL (200 µg apoB/mL) isolated from a pool of plasma from healthy volunteers were incubated with 4 µM CuSO₄ and the formation of hydroperoxides was monitored for 2 h. Ferric products generated from hydroperoxides were measured as xylenol orange complexes at 560 nm [21]. Butylated hydroxytoluene (BHT) and curcumin (powerful antioxidants) were used as positive controls for the inhibition of LDL oxidation. Results reported in Figure 1A show that *D. apetalum* and *A. borbonica* extracts significantly reduced the formation of copper-induced LDL hydroperoxides at 50 and 100 µM GAE, while curcumin significantly exerted its antioxidant effect at all concentrations tested (25, 50 and 100 µM). *D. apetalum* extract is significantly more efficient at 50 µM GAE than *A. borbonica* extract.

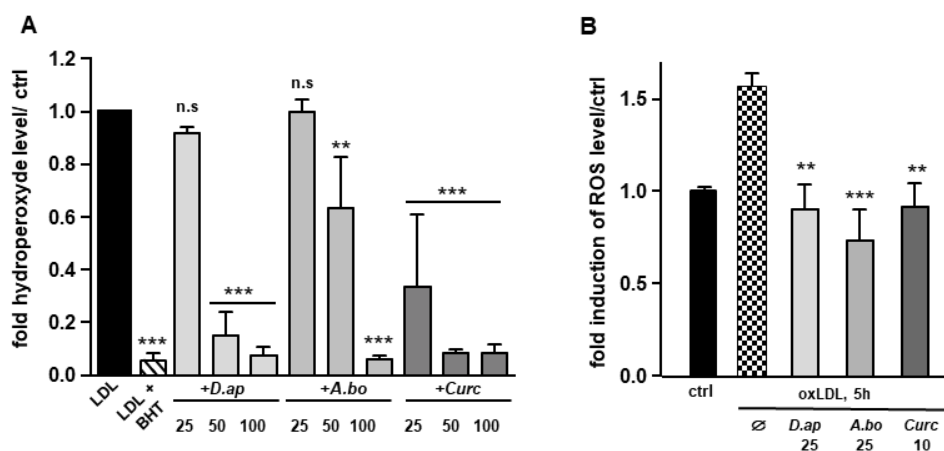


Figure 1. *D. apetalum* and *A. borbonica* extracts exhibit antioxidant properties. Antioxidant properties of various concentrations of polyphenol-rich extracts from *D. apetalum* and *A. borbonica* or curcumin were evaluated on LDL oxidation and oxLDL-induced intracellular ROS production in HMEC-1 cells. (A) Fold increase of hydroperoxide formation assayed by xylenol orange test. LDL are incubated for 2 h at 37 °C with 4 µM CuSO₄ with or without plant extracts. Hydroperoxide formation was followed by colorimetric reaction, using xylenol orange; (B) inhibition of oxLDL-induced intracellular ROS production. HMEC-1 cells were pre-treated with plant extracts 2 h before addition of oxLDLs for 5 h. Increase in intracellular ROS was quantified using H₂DCFDA fluorescent probe and

expressed as fold of induction of ROS levels compared with that of control (without oxLDLs). Results are expressed as means \pm SEM of at least 3 independent experiments. ** $p < 0.01$, *** $p < 0.001$, compared to control (ctrl) (LDL) [A]; ** $p < 0.01$, *** $p < 0.001$, compared to oxLDLs [B] using one-way ANOVA with posthoc Tukey's test.

Vascular cells and particularly endothelial cells produce ROS, promoting LDL oxidation [22]. We tested the capacity of plant extracts to limit cell-induced LDL oxidation. Both polyphenol-rich extracts (10–50 μ M GAE) and curcumin (5–10 μ M) were able to significantly prevent TBARS formation in cell-incubated LDL (50 μ g apoB/mL) (Table 5). Altogether, these results demonstrate that *A. borbonica* and *D. apetalum* extracts exhibit a robust free radical-scavenging activity against both copper- and cell-induced LDL oxidation.

Table 5. *D. apetalum* and *A. borbonica* plant extracts prevent lipid peroxidation.

	TBARS (μ M)	TBARS (μ M)	<i>p</i>	TBARS (μ M)	<i>p</i>	TBARS (μ M)	<i>p</i>
	control	10 μ M		25 μ M		50 μ M	
<i>D. apetalum</i>	4.210 \pm 0.710	0.046 \pm 0.011	< 0.001	0.023 \pm 0.012	< 0.001	0.027 \pm 0.014	< 0.001
<i>A. borbonica</i>	3.578 \pm 0.188	0.042 \pm 0.003	< 0.001	0.019 \pm 0.007	< 0.001	0.025 \pm 0.011	< 0.001
	control	1 μ M		5 μ M		10 μ M	
Curcumin	3.742 \pm 0.572	3.141 \pm 0.621	n.s	0.130 \pm 0.031	< 0.001	0.031 \pm 0.011	< 0.001

Serum-starved HMEC-1 cells were preincubated or not (control, vehicle PBS) for 2 h with plant extracts (10, 25 or 50 μ M) or curcumin (1, 5 or 10 μ M) before addition of 200 μ g apoB/mL of LDL for 6 h. Lipid peroxidation was measured in conditioned medium by TBARS assay and expressed as μ M of MDA. All data are expressed as means \pm SEM of at least three independent experiments. n.s: nonsignificant.

3.3. Oxidative Stress and Antioxidant Response Induced by oxLDLs in Endothelial Cells Are Inhibited by *A. Borbonica* and *D. Apetalum* Extracts

OxLDLs induce an intense oxidative stress in vascular cells [14,23,24]. The capacity of *A. borbonica* and *D. apetalum* extracts to limit oxLDL-induced generation of ROS was evaluated in HMEC-1 cells. OxLDL induced a 1.55-fold increase in ROS production respectively after 5 h of HMEC-1 cells stimulation. Both polyphenol-rich extracts exhibited a significant antioxidant activity similar to that of curcumin, used as a positive control (Figure 1B). Interestingly, after 5 h of treatment of cells with oxidized LDL, *A. borbonica* extract displayed a more significant antioxidant effect than *D. apetalum* extract. We then tested whether the polyphenol extracts interfered with LDL binding and/or uptake using fluorescently labeled lipoproteins (Figure S1, see supplemental data). No significant difference in LDL uptake was observed when HMEC-1 cells were coincubated or not with 25 μ M GAE of plant extracts, or with 10 μ M of curcumin.

When exposed to an oxidative stimulus such as oxLDLs, endothelial cells trigger an antioxidant response by stimulating the production of enzymes in charge of O_2^- and H_2O_2 detoxification, namely superoxide dismutase (SOD) and catalase, respectively. As shown in Figure 2, both catalase and SOD activities were increased after HMEC-1 cells incubation with oxLDLs. In the presence of plant extracts, the antioxidant response was no longer observed, suggesting that *A. borbonica* and *D. apetalum* extracts inhibit the oxidative stress generated by oxLDLs, upstream of the induction of SOD and catalase activities.

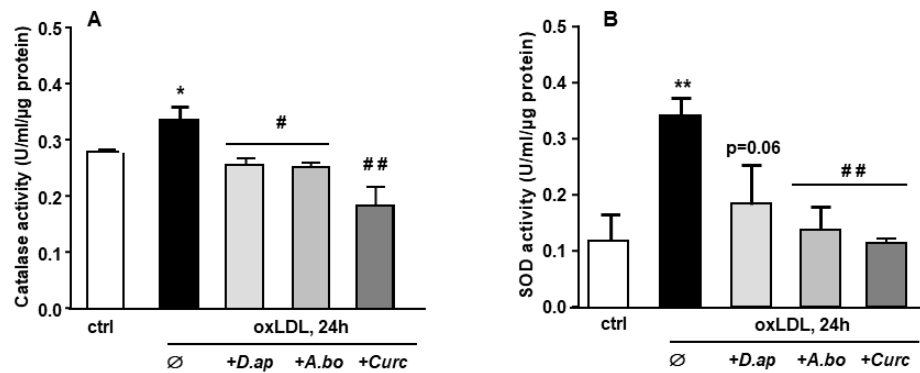


Figure 2. *D. apetalum* and *A. borbonica* extracts prevent oxLDL-induced cellular oxidative stress. Effects of polyphenol-rich extracts from *D. Apetalum* and *A. borbonica* or curcumin on antioxidant activity of oxLDL-stimulated HMEC-1 cells. Subconfluent serum-starved HMEC-1 cells were preincubated for 2 h with *D. apetalum* (25 μM), *A. borbonica* (25 μM) polyphenol-rich extracts or curcumin (10 μM) before addition of oxLDLs (200 μg apoB/mL) for an additional 12 h. (A) Catalase and (B) total SOD activities were expressed as catalytic units per μg of proteins as means ± SEM of at least 3 independent experiments. * $p < 0.05$; ** $p < 0.01$ compared to control (ctrl, vehicle PBS); # $p < 0.05$; ## $p < 0.01$ compared to oxLDLs were calculated using one-way ANOVA with Tukey's posthoc test.

3.4. *A. Borbonica* and *D. Apetalum* Extracts Inhibit the Cytotoxic Effects of oxLDLs on Endothelial Cells

OxLDLs are well documented for their cytotoxic effects on endothelial cells [5,25]. We tested the ability of *A. borbonica* and *D. apetalum* extracts to limit apoptosis induced by oxLDLs under our experimental conditions. Different techniques were used to quantify the overall cell viability and specifically apoptosis, including the MTT reduction by the respiratory chain and other electron transport systems, which serve as an estimate for the metabolic activity of living cells, the cell membrane permeability (propidium iodide, PI), morphological nuclear changes (SYTO 13), phosphatidylserine exposure (annexin V membrane binding), cytochrome C release and caspase 3 activation. The MTT test showed that extracts of *A. borbonica* (10–50 μM) and *D. apetalum* (25–50 μM) together with curcumin (10 μM) limited oxLDL-induced mitochondrial dysfunction (Figure 3A–C). This suggests that both plant extracts exhibited a cytoprotective effect capable of counteracting oxLDL toxicity for concentrations as low as 10 μM GAE for *A. borbonica* and 25 μM GAE for *D. apetalum*.

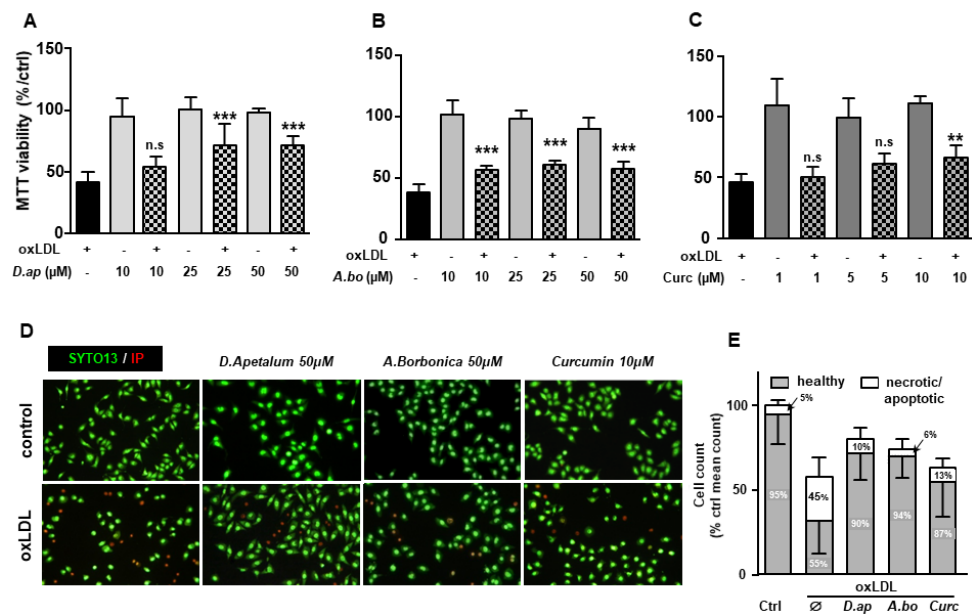


Figure 3. *D. apetalum* and *A. borbonica* extracts exert cytoprotective effects on oxLDL-stimulated HMEC-1 cells. Analysis of cell viability in HMEC-1 cells was evaluated by MTT assay. Subconfluent serum-starved HMEC-1 cells were preincubated for 2 h with (A) *D. apetalum* (10–50 µM), (B) *A. borbonica* (10–50 µM) and (C) curcumin (1–10 µM) before addition of oxLDLs (200 µg apoB/mL), for 24 h. MTT reduction and cell viability was analyzed as described. Results are expressed as percentage of untreated control cells (vehicle, PBS) and represent mean ± SEM of 4 independent experiments. (D) SYTO-13/PI staining of HMEC-1 cells pretreated with plant extracts or curcumin followed by addition of oxLDLs (200 µg apoB/mL, for 24 h), images show protective effect of plant extracts and curcumin towards oxLDL-induced apoptosis. (E) Living, apoptotic, and necrotic cells were counted after staining by SYTO-13/PI as described. Results are expressed as percentage and represent mean ± SEM of at least 4 independent experiments. ** $p < 0.01$; *** $p < 0.001$ were calculated using one-way ANOVA with Tukey's post hoc test. n.s.: nonsignificant.

The plant extracts also significantly reduced apoptosis and necrosis as shown by various tests. Using SYTO 13/PI staining, nuclear morphology and membrane integrity could be assessed simultaneously. SYTO 13 is a green, fluorescent nucleic acid dye shown to stain live cells (Figure 3D). OxLDLs induced a nuclear condensation and fragmentation, accompanied by cell shrinkage, and eventually increased membrane permeability. In Figure 3E, the total number of adherent cells was significantly decreased upon incubation with oxLDLs (42% decrease, $p < 0.001$ relative to control cells). Among the remaining adherent cells, apoptosis and postapoptotic necrosis features were observed in oxLDL-treated cells (about 45 % of remaining cells) whereas pre-treatment of endothelial cells with the plant extracts significantly limited this proapoptotic effect of oxLDLs (10.0 % and 5.8 % of remaining cells with *D. apetalum* and *A. borbonica* respectively, ($p < 0.001$ relative to oxLDL), and 12.7 % of remaining cells with curcumin ($p < 0.05$ relative to oxLDLs) (Figure 3E). This result was further confirmed by quantifying annexin-V staining, which was significantly limited by pre-incubation with the plant extracts, whereas curcumin only partially reduced the effects of oxLDLs (Figure 4). We previously demonstrated that the mechanism of apoptosis triggered by oxLDLs involved an intrinsic mitochondrial pathway leading to caspase 3 activation [15]. As shown in Figure 5, immunofluorescence staining revealed the localization of cytochrome C in mitochondria in untreated control cells, whereas after oxLDL treatment we observed a perinuclear and cytosolic relocation of the cytochrome C. Importantly, the release of the cytochrome C from mitochondria to cytosol is prevented by the pre-treatment of endothelial cells with the plant extracts and curcumin.

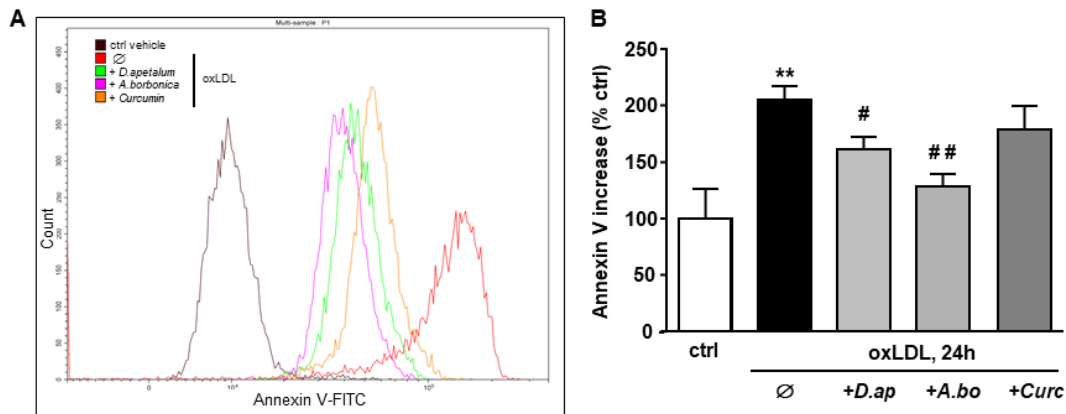


Figure 4. *D. apetalum* and *A. borbonica* extracts prevent oxLDL-induced phosphatidylserine exposure. Subconfluent serum-starved HMEC-1 cells were preincubated for 2 h with *D. apetalum* (25 μ M), *A. borbonica* (25 μ M) polyphenol-rich extracts or curcumin (10 μ M) before addition of oxLDLs (200 μ g apoB/mL) for an additional 24 h. (A) Illustration of detection of Annexin V binding in HMEC-1 cells quantified by flow cytometry using Annexin V-FITC probe. (B) Graph represents percentage of Annexin V fluorescence relative to untreated control HMEC-1 cells (vehicle PBS) in each condition. Results are expressed as means \pm SEM of 3 independent experiments. ** $p < 0.01$ vs. control (ctrl); # $p < 0.05$; ## $p < 0.01$ vs. oxLDL using one-way ANOVA with Tukey's posthoc test.

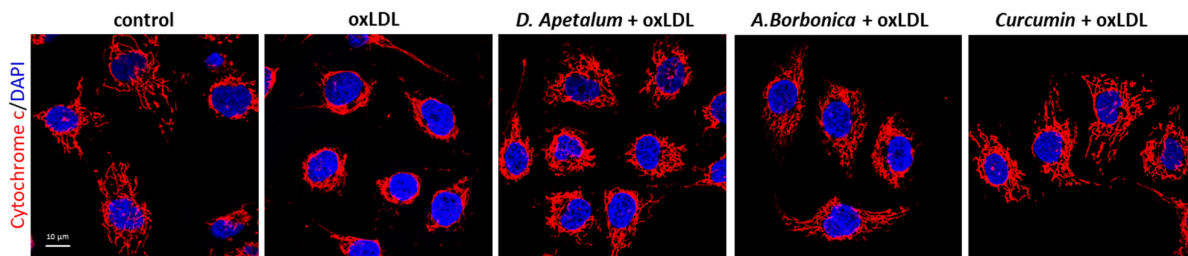


Figure 5. *D. apetalum* and *A. borbonica* extracts inhibit oxLDL-induced cytochrome C release from mitochondria to cytosol. Subconfluent serum-starved HMEC-1 cells were preincubated for 2 h with *D. apetalum* (25 μ M), *A. borbonica* (25 μ M) polyphenol-rich extracts or curcumin (10 μ M) before addition of oxLDLs (200 μ g apoB/mL) for an additional 24 h, control condition corresponds to untreated HMEC-1 cells (vehicle, PBS). Images are representative of immunofluorescence staining of cytochrome C (red) and cell nuclei (blue) stained with DAPI. Scale bar = 10 μ m.

Finally, caspase 3 activation and DNA fragmentation (determined by the TUNEL method), both characteristics of the late apoptotic process, were increased by incubation with oxLDLs and significantly reduced by pretreatment with *A. borbonica* extract and curcumin (Figures 6 and 7).

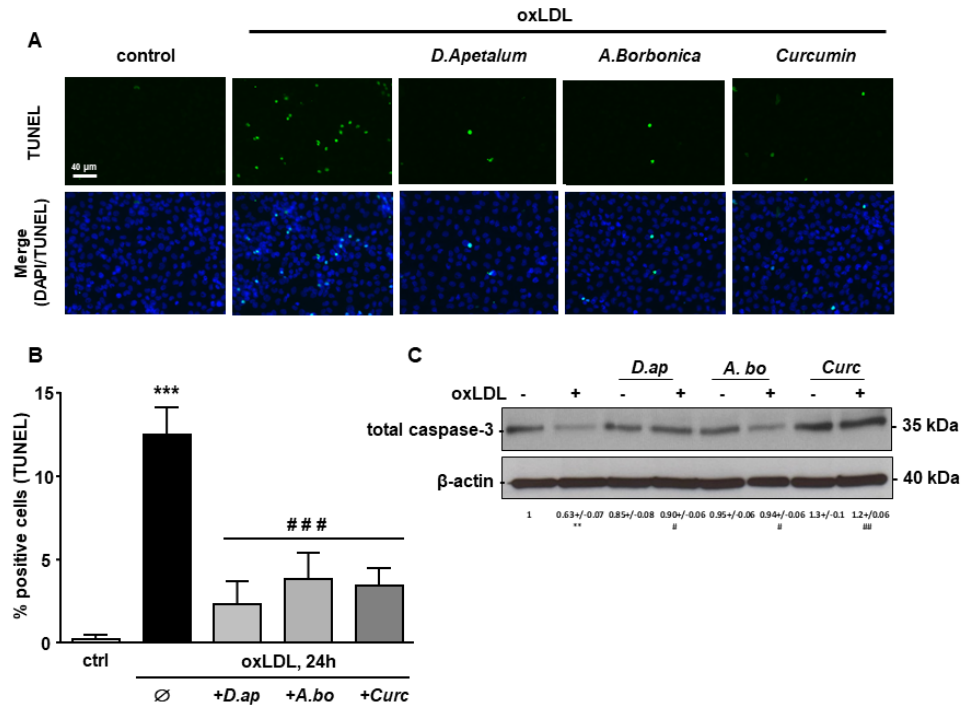


Figure 6. *D. apetalum* and *A. borbonica* extracts inhibit oxLDL-induced caspase 3 activation. Subconfluent serum-starved HMEC-1 cells were preincubated for 2 h with *D. apetalum* (25 μ M), *A. borbonica* (25 μ M) polyphenol-rich extracts or curcumin (10 μ M) before addition of oxLDLs (200 μ g apoB/mL) for an additional 24 h. (A) Immunofluorescence staining of cleaved caspase-3 expression in HMEC-1 cells. Green signal represents cleaved caspase-3 levels. Cell nuclei are stained with DAPI (blue). Scale bar = 40 μ m; (B) graph represents means \pm SD of cleaved caspase-3 fluorescence intensity. Results are expressed as means \pm SEM of three independent experiments. (C) Western-blot analysis of total caspase-3 expression in HMEC-1 cells. Densitometric analyses of expression level of caspase-3 protein upon different conditions are indicated. data are expressed as mean \pm SEM of four independent experiments. *** $p < 0.001$ vs. control; ### $p < 0.001$ vs. oxLDL using one-way ANOVA with Tukey’s posthoc test.

Our results demonstrate that polyphenol-rich extracts exerted a potent cytoprotective effect on endothelial cells exposed to oxLDLs, suggesting that they could limit the atherogenic process.

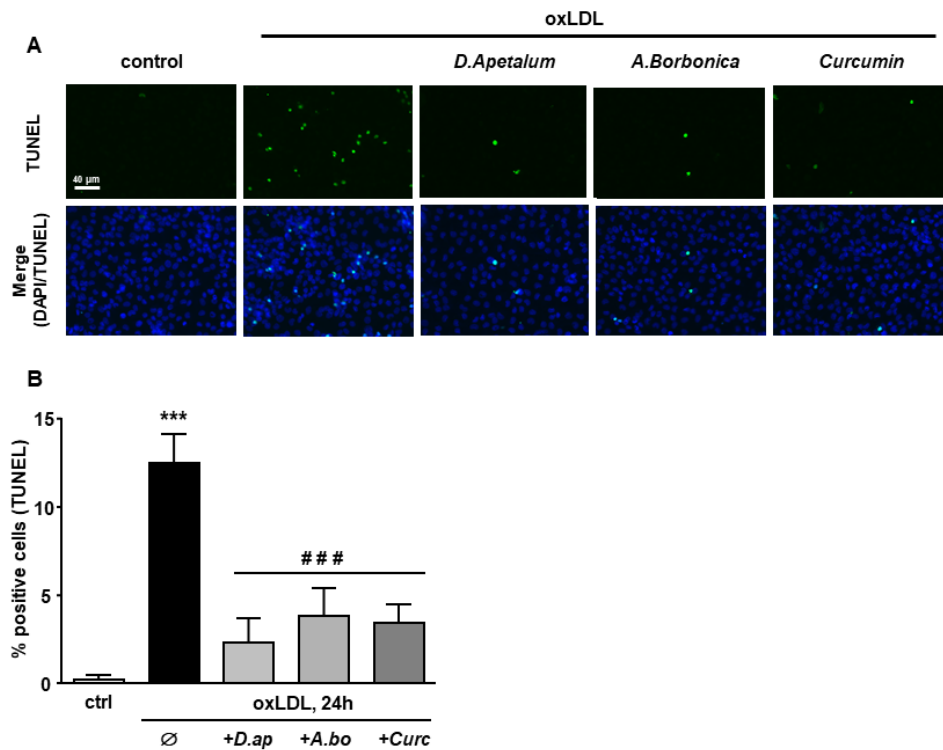


Figure 7. *D. apetalum* and *A. borbonica* extracts limit oxLDL-induced DNA fragmentation. Subconfluent serum-starved HMEC-1 cells were preincubated for 2 h with *D. apetalum* (25 μM), *A. borbonica* (25 μM) polyphenol-rich extracts or curcumin (10 μM) before addition of oxLDLs (200 μg apoB/mL) for an additional 24 h. (A) Analysis of DNA fragmentation by TUNEL assay in HMEC-1 cells (green). Cell nuclei are stained with DAPI (blue). Scale bar = 40 μm; (B) graph represents percentage of TUNEL-positive cells. Results are expressed as means ± SEM of 3 independent experiments; *** $p < 0.001$ vs. control (ctrl); ### $p < 0.001$ vs. oxLDL using one-way ANOVA with Tukey's posthoc test.

4. Discussion

Taken together, our data demonstrate that *A. borbonica* and *D. apetalum* medicinal plant extracts as well as curcumin efficiently inhibit LDL oxidation and could potentially limit intracellular oxidative stress in endothelial cells after exposition to oxLDLs. In addition, the polyphenol-rich extracts of both plants exerted a significant cytoprotective effect as shown by various assays including MTT reduction, SYTO 13/propidium iodide staining, annexin V exposure, caspase 3 activation and TUNEL. For the first time, the antiapoptotic effects against oxLDL-induced toxicity are reported for these plant extracts.

In Reunion Island, medicinal plants are widely used for their anti-inflammatory, antidiabetic, diuretic, or dermatological properties either as herbal tea (infusion or decoction) or in external use (skin application). *A. borbonica* is referenced at the French pharmacopeia for its healing and hemostatic properties, but is widely used as herbal tea. *D. apetalum* is also used against skin irritation (added to the bath). Polyphenol-rich extracts from both plants were shown to contain high amounts of these antioxidants [11]; the antioxidant activity of *A. borbonica* was reported for many years [26]. The present study is the first to evaluate the potential of these medicinal plants from Reunion Island to limit LDL oxidation and subsequent cytotoxic effects on endothelial cells. The polyphenol composition of *D. apetalum* and *A. borbonica* was previously published by our laboratory [11]. Both plant extracts have in common kaempferol-*O*-hexoside-*O*-rhamnoside but have different compositions regarding other major polyphenols. Indeed, *A. borbonica* contains mainly caffeic acid and dicaffeoylquinic acids whereas *D. apetalum* contains procyanidins

including dimer type A/B and trimer type A, coumaric acid, epicatechin, quercetin-*O*-rutinoside, kaempferol 3-*O*-hexoside. Most of these compounds were previously reported to inhibit LDL oxidation. For example, chlorogenic acid reacts with peroxy radicals to limit LDL oxidation [27], and can be incorporated into LDL after drinking polyphenol-containing beverages such as coffee, thereby increasing the resistance of LDL to oxidation [28]. Chlorogenic acid was also reported to protect against atherosclerosis in ApoE KO mice [29]. Procyanidin moieties were shown to limit LDL oxidation, regardless of their molecular weight for monomers, dimers, and trimers whereas hexamers are less effective [30]. Other polyphenols such as flavonoids including epicatechin, quercetin and kaempferol also exhibit radical-scavenging effects and are important inhibitors of LDL oxidation [31]. Curcumin was shown to inhibit LDL oxidation both *in vitro* [10,32] and *in vivo*, after oral administration in a rabbit model of atherosclerosis [33].

Even if *in vivo* polyphenol bioavailability may depend on the interindividual variability and may differ from one polyphenol to another, circulating polyphenol concentrations reach the range of μM . The doses selected in the present study were 25, 50, and 100 μM for plant polyphenols, and 1, 5 and 10 μM for curcumin. Although these doses are higher than the physiological concentrations reported in nutritional interventions, such pharmacological concentrations were broadly used in similar experiments in the literature [18,34] as well as in our published studies using *D. apetalum* and *A. borbonica* polyphenols [11,12] or pure polyphenols like curcumin [35,36]. Higher curcumin concentrations (12.5–100 μM) were reported to induce cell death in endothelial cells [37].

Specific polyphenols such as epicatechin and its derivatives procyanidins were identified in *D. apetalum* while specific caffeic acid esters were detected in *A. borbonica*. In parallel, both plant extracts exhibited similar polyphenols such as kaempferol or quercetin recognized as a flavonoid exerting a strong antioxidant effect due to its B-ring hydroxylation that facilitates electron delocalization on the aromatic ring [38]. Here, the similar effects induced by both plant extracts may result from the presence of similar potent antioxidant polyphenols such as quercetin. Moreover, we used similar doses of total polyphenols from both plant extracts. This may contribute to a similar antioxidant capacity of both extracts as we previously demonstrated through DPPH radical-scavenging activity assay for *D. apetalum* and *A. borbonica* [11]. Concerning the antioxidant potential of a polyphenol, it may depend on the structure of the polyphenol considered, but also on the experimental method used. In the study by Hatia et al. [35], we compared by different *in vitro* assays the antioxidant capacity of 26 polyphenols including epicatechin, caffeic acid, or quercetin found in the two plant extracts. We found that all polyphenols tested at the same dose exerted antioxidant effects, but the magnitude of the antioxidant capacity depended on the method used. For instance, epicatechin and quercetin exerted a similar reducing activity via Folin–Ciocalteu assay. Epicatechin and caffeic acid exhibited a similar radical-scavenging property with DPPH assay. Quercetin and caffeic acid have a close radical-scavenging capacity, as assessed by the Trolox test. Thus, despite the difference in polyphenolic composition of the plant extracts, the use of similar doses of total polyphenols may contribute to explain the similar effects of plant extracts.

We previously demonstrated that oxLDLs are capable of inducing cytotoxic effects in a variety of cell type including endothelial cells [5,25]. These cytotoxic effects have also been shown to be inhibited by various antioxidant strategies such as polyphenols supplementation [39]. Other studies have shown that polyphenol-rich plant extracts, such as those from *Hibiscus sabdariffa* leaf, can inhibit oxLDL-induced endothelial cell apoptosis via an upregulation of the autophagic pathway. In particular, epicatechin gallate contained in this extract was found to be responsible for this protective effect [40].

In bovine aortic endothelial cells, oxLDLs were able to induce a significant intracellular oxidative stress induced as early as 5 min after stimulation, reaching a plateau after 30–45 min, via an interaction with LOX-1 (Lectin-like oxLDL receptor) [23]. Similarly, Yen et al. reported H_2O_2 generation measured after 30 min of oxLDL incubation with HUVECs. OxLDLs used in the present study may utilize, at least in part, the classical internalization

pathway via the LDL receptor since oxidative modifications of proteins and lipids are not sufficient to fully direct these lipoproteins towards scavenger receptors [41]. After binding to their receptors, oxLDLs are internalized into endosomes and then lysosomes in which oxidatively modified products can diffuse into the cytosol. Intracellular ROS formation from peroxisomes, NADPH oxidase, mitochondrial respiratory chain and lipoxygenases is then observed. Various signaling pathways are then activated, leading to an intracellular calcium peak, mitochondrial intrinsic pathway activation and subsequent changes in the expression of pro- and anti-apoptotic genes [14,42,43]. Other genes involved in the antioxidant defense can also be induced [7]. Lipid peroxides such HPODE and HODE (13-hydroperoxyoctadecadienoic and 13-hydroxyoctadecadienoic acids, respectively) that can be found in oxLDLs and were reported to induce the expression of catalase [44].

In the present study, we report an increase in intracellular H₂O₂ formation assessed by H₂DCFHDA fluorescence at 1 and 5 h after stimulation with oxLDLs. It is suggested that the intracellular oxidative stress induced by oxLDLs and inhibited by both plant extracts and curcumin may be upstream of the cytotoxic cascade. Literature data report that antioxidant effects of polyphenols may result from different mechanisms involving the direct neutralization of ROS, or indirectly through the modulation of ROS-producing and ROS-detoxifying enzymes [45]. Firstly, due to their phenolic structure, polyphenols are able to directly scavenge and reduce free radicals. In the case of polyphenols from *D. apetalum* and *A. borbonica*, such radical-scavenging and reducing capacities were already demonstrated in our previous studies [11,12]. Secondly, polyphenols from *D. apetalum* and *A. borbonica* may exert antioxidant properties through their ability to modulate the production of redox enzymes [45]. In endothelial cell models, we previously showed that *A. borbonica* polyphenols improved intracellular ROS levels, the expression of genes encoding NOX4, GPx or HO1 as well as Cu/Zn antioxidant activity deregulated by oxidative stress conditions [46,47]. *D. apetalum* polyphenols were also found to improve mitochondrial molecular targets involved in redox status in endothelial cell model during oxidative stress conditions [48]. Both the transcriptional factors Nrf2 and NFκB play opposite pivotal roles in the regulation of the production of redox enzymes. In endothelial cell model exposed to oxidative stress conditions, we reported that *A. borbonica* polyphenols helped to preserve the antioxidant defense system by reducing the nuclear translocation of Nrf2 and elevating Nrf2 gene expression [46]. In parallel, *A. borbonica* polyphenols counteracted the elevation of NFκB activity and gene expression mediated by oxidative stress [47,49]. Altogether, these findings provide evidence for the several possible mechanisms of action of antioxidant polyphenols from *D. apetalum* and *A. borbonica* plants. In the present study, the ability of plant polyphenols to improve redox targets such as catalase and SOD activities or intracellular ROS levels deregulated by ox-LDL, may involve these several possible mechanisms of action.

The bioavailability of polyphenols and their cellular distribution are not clearly demonstrated, in particular whether they accumulate within endothelial cells and via which potential receptor [50]. Using a cerebral endothelial cell line (bEnd.3), we recently demonstrated that caffeic acid, quercetin and its methylated metabolite isorhamnetin could accumulate intracellularly whereas chlorogenic and gallic acids were only able to bind the plasma membrane [49]. Quercitrin, a glycoside formed from quercetin and rhamnose, showed potential to block oxLDL uptake, suggesting that some polyphenol could act at the extracellular level [51]. Similarly, procyanidins were shown to be potent inhibitors of LOX-1 / oxLDL interactions [52]. In our study, the uptake of LDLs is not modified in the presence of plant extracts, suggesting that the protective effects are not mediated by potential interference between polyphenols and LDL receptors during coinubation.

Some recent studies suggest that polyphenols can be transported across the blood-brain barrier and exert their protective effects via the mTOR signaling pathway [53]. Resveratrol was shown to be taken up by endothelial cells via both passive and active transport involving SGLT-1 (sodium-dependent glucose transporter 1) [54]. In our study,

the mechanism of action of the plant extracts remains to be elucidated and it is not excluded that the different polyphenols act at both the extracellular and intracellular levels.

Endothelial dysfunction is a hallmark of atherogenesis that is involved in all stages from initial lipid accumulation to plaque rupture [55]. Mildly oxLDLs were shown to induce massive apoptosis of endothelial cells via activation of various intracellular proapoptotic signaling pathways, ultimately leading to DNA fragmentation and cell detachment [25]. Here, we demonstrated that plant extracts were able to prevent oxLDL-induced endothelial cell apoptosis using different assays to evaluate apoptosis (annexin V exposure, cytochrome C release caspase 3 activation, TUNEL, nuclear morphology, membrane permeability). Several studies reported the endothelial protective effects of different polyphenols against oxLDL cytotoxicity. Resveratrol cytoprotection is particularly documented [56–58] but other polyphenols were demonstrated to limit the deleterious effects of oxLDLs [40,59]. The intracellular signaling pathway involved in polyphenol protection may involve PI3K/Akt/eNOS [59]. In our study, we did not investigate the potential intracellular pathway that might be the target of polyphenols. However, it is likely that plant extracts exert their protective effect at different levels. In addition to the expected antioxidant effect, polyphenols might act after the initiation of intracellular oxidative stress because they remained cytoprotective even when added up to 12 h after oxLDLs (data not shown). This suggests that other targets of the apoptotic cascade could be modulated by polyphenol-rich plant extracts. For example, resveratrol was reported to activate SIRT-1, which in turn can modulate proteins involved in cell survival and cell cycle arrest [60]. The exact mechanism by which polyphenol-rich extracts of *A. borbonica* and *D. apetalum* inhibit endothelial cell apoptosis requires further investigation; firstly, to identify the molecules responsible for this protective effect, and secondly, to unveil the involved intracellular signaling pathway.

5. Conclusions

Our study shows for the first time that polyphenol-rich extracts from two original medicinal plants from Reunion Island exhibit potent antioxidant and antiapoptotic effects in response to oxLDLs on vascular endothelial cells. The potential use of these plants for prevention of atherosclerosis should be investigated in appropriate preclinical models.

Supplementary Materials: The following supporting information can be downloaded at: www.mdpi.com/2076-3921/11/1/34/s1, Figures S1 and S2: Identification of polyphenols from *D. Apetalum* and *A. Borbonica* plant extracts by mass spectroscopy. Figure S3: LDL uptake is not prevented by pre-incubation of *D. apetalum* and *A. Borbonica* in HMEC-1 cells.

Author Contributions: Conceptualization: C.V. and O.M.; experiment investigation and methodology: J.B., P.R., and J.F.; phenolic compounds identification by mass spectroscopy: B.V.; writing—original draft preparation: C.V., P.R., and O.M.; figures design and conception: J.B. and P.R.; writing—review and editing: C.V., P.R., M.-P.G. and O.M. All authors have read and agreed to the published version of the manuscript.

Funding: This work was supported by the Ministère de l'Enseignement Supérieur et de la Recherche, the Université de La Réunion, the "Structure fédérative de recherche biosécurité en milieu tropical (BIOST)" and by the European Regional Development Funds RE0001897 (EU- Région Réunion -French State national counterpart). JB is a recipient of a fellowship grant from Région Réunion, de l'Enseignement Supérieur et de la Recherche, La Réunion University.

Institutional Review Board Statement: Not applicable.

Informed Consent Statement: Not applicable.

Data Availability Statement: All of the data is contained within the article and the supplementary materials

Conflicts of Interest: The authors declare no conflict of interest.

References

1. Quinn, M.T.; Parthasarathy, S.; Fong, L.G.; Steinberg, D. Oxidatively modified low density lipoproteins: A potential role in recruitment and retention of monocyte/macrophages during atherogenesis. *Proc. Natl. Acad. Sci. USA* **1987**, *84*, 2995–2998. <https://doi.org/10.1073/pnas.84.9.2995>.
2. Balla, G.; Jacob, H.S.; Eaton, J.W.; Belcher, J.D.; Vercellotti, G.M. Hemin: A possible physiological mediator of low density lipoprotein oxidation and endothelial injury. *Arter. Thromb. A J. Vasc. Biol.* **1991**, *11*, 1700–1711. <https://doi.org/10.1161/01.atv.11.6.1700>.
3. Khan, B.V.; Parthasarathy, S.S.; Alexander, R.W.; Medford, R.M. Modified low density lipoprotein and its constituents augment cytokine-activated vascular cell adhesion molecule-1 gene expression in human vascular endothelial cells. *J. Clin. Investig.* **1995**, *95*, 1262–1270. <https://doi.org/10.1172/jci117776>.
4. Ho-Tin-Noé, B.; Le Dall, J.; Gomez, D.; Louedec, L.; Vranckx, R.; El-Bouchtaoui, M.; Legrès, L.; Meilhac, O.; Michel, J.B. Early Atheroma-Derived Agonists of Peroxisome Proliferator-Activated Receptor-Gamma Trigger Intramedial Angiogenesis in a Smooth Muscle Cell-Dependent Manner. *Circ. Res.* **2011**, *109*, 1003–1014.
5. Nègre-Salvayre, A.; Pieraggia, M.T.; Mabile, L.; Salvayrea, R. Protective Effect of 17 Beta-Estradiol against the Cytotoxicity of Minimally Oxidized Ldl to Cultured Bovine Aortic Endothelial Cells. *Atherosclerosis* **1993**, *99*, 207–217.
6. Reid, V.C.; Mitchinson, M.J.; Skepper, J.N. Cytotoxicity of oxidized low-density lipoprotein to mouse peritoneal macrophages: An ultrastructural study. *J. Pathol.* **1993**, *171*, 321–328. <https://doi.org/10.1002/path.1711710413>.
7. Parthasarathy, S.; Santanam, N.; Ramachandran, S.; Meilhac, O. Oxidants and antioxidants in atherogenesis. An appraisal. *J. Lipid Res.* **1999**, *40*, 2143–57.
8. Saita, E.; Kondo, K.; Momiyama, Y. Anti-Inflammatory Diet for Atherosclerosis and Coronary Artery Disease: Antioxidant Foods. *Clin. Med. Insights: Cardiol.* **2014**, *8* (Suppl. 3), CMC-S17071. <https://doi.org/10.4137/cmc.s17071>.
9. Scalbert, A.; Williamson, G. Dietary Intake and Bioavailability of Polyphenols. *J. Nutr.* **2000**, *130*, 2073S–2085S. <https://doi.org/10.1093/jn/130.8.2073s>.
10. Naidu, K.A.; Thippeswamy, N. Inhibition of human low density lipoprotein oxidation by active principles from spices. *Mol. Cell. Biochem.* **2002**, *229*, 19–23. <https://doi.org/10.1023/a:1017930708099>.
11. Marimoutou, M.; Le Sage, F.; Smadja, J.; d’Hellencourt, C.L.; Gonthier, M.P.; Robert-Da Silva, C. Antioxidant Polyphenol-Rich Extracts from the Medicinal Plants *Antirhea Borbonica*, *Doratoxylon Apetalum* and *Gouania Mauritiana* Protect 3t3-L1 Preadipocytes against H₂O₂, Tnfa and Lps Inflammatory Mediators by Regulating the Expression of Superoxide Dismutase and Nf-Kappab Genes. *J. Inflamm.* **2015**, *12*, 1–15.
12. Le Sage, F.; Meilhac, O.; Gonthier, M.-P. Anti-inflammatory and antioxidant effects of polyphenols extracted from *Antirhea borbonica* medicinal plant on adipocytes exposed to *Porphyromonas gingivalis* and *Escherichia coli* lipopolysaccharides. *Pharmacol. Res.* **2017**, *119*, 303–312. <https://doi.org/10.1016/j.phrs.2017.02.020>.
13. Delveaux, J.; Turpin, C.; Veeren, B.; Diotel, N.; Bravo, S.B.; Begue, F.; Álvarez, E.; Meilhac, O.; Bourdon, E.; Rondeau, P. *Antirhea borbonica* Aqueous Extract Protects Albumin and Erythrocytes from Glycoxidative Damages. *Antioxidants* **2020**, *9*, 415. <https://doi.org/10.3390/antiox9050415>.
14. Vindis, C.; Elbaz, M.; Escargueil-Blanc, I.; Augé, N.; Heniquez, A.; Thiers, J.-C.; Negre-Salvayre, A.; Salvayre, R. Two Distinct Calcium-Dependent Mitochondrial Pathways Are Involved in Oxidized LDL-Induced Apoptosis. *Arter. Thromb. Vasc. Biol.* **2005**, *25*, 639–645. <https://doi.org/10.1161/01.atv.0000154359.60886.33>.
15. Yagi, K. Simple Assay for the Level of Total Lipid Peroxides in Serum or Plasma. *Free Radic. Antioxid. Protoc.* **1998**, *108*, 101–106. <https://doi.org/10.1385/0-89603-472-0:101>.
16. Jiang, Z.-Y.; Hunt, J.V.; Wolff, S.P. Ferrous ion oxidation in the presence of xylenol orange for detection of lipid hydroperoxide in low density lipoprotein. *Anal. Biochem.* **1992**, *202*, 384–389. [https://doi.org/10.1016/0003-2697\(92\)90122-n](https://doi.org/10.1016/0003-2697(92)90122-n).
17. Jiang, Z.-Y.; Woollard, A.C.S.; Wolff, S.P. Lipid hydroperoxide measurement by oxidation of Fe²⁺ in the presence of xylenol orange. Comparison with the TBA assay and an iodometric method. *Lipids* **1991**, *26*, 853–856. <https://doi.org/10.1007/bf02536169>.
18. Muller, C.; Salvayre, R.; Negre-Salvayre, A.; Vindis, C. HDLs inhibit endoplasmic reticulum stress and autophagic response induced by oxidized LDLs. *Cell Death Differ.* **2010**, *18*, 817–828. <https://doi.org/10.1038/cdd.2010.149>.
19. Larroque-Cardoso, P.; Swiader, A.; Ingueneau, C.; Nègre-Salvayre, A.; Elbaz, M.; Reyland, M.E.; Salvayre, R.; Vindis, C. Role of Protein Kinase C Delta in Er Stress and Apoptosis Induced by Oxidized Ldl in Human Vascular Smooth Muscle Cells. *Cell Death Dis.* **2013**, *4*, e520.
20. Salvayre, R.; Vindis, C.; Ingueneau, C.; Athias, A.; Marcheix, B.; Huynh-Do, U.; Gambert, P.; Nègre-Salvayre, A. TRPC1 is regulated by caveolin-1 and is involved in oxidized LDL-induced apoptosis of vascular smooth muscle cells. *J. Cell Mol. Med.* **2009**, *13*, 1620–1631. <https://doi.org/10.7892/boris.28095>.
21. Gay, C.; Collins, J.; Gebicki, J.M. Hydroperoxide Assay with the Ferric–Xylenol Orange Complex. *Anal. Biochem.* **1999**, *273*, 149–155. <https://doi.org/10.1006/abio.1999.4208>.
22. Mabile, L.; Meilhac, O.; Escargueil-Blanc, I.; Trolly, M.; Pieraggi, M.-T.; Salvayre, R.; Nègre-Salvayre, A. Mitochondrial Function Is Involved in LDL Oxidation Mediated by Human Cultured Endothelial Cells. *Arter. Thromb. Vasc. Biol.* **1997**, *17*, 1575–1582. <https://doi.org/10.1161/01.atv.17.8.1575>.

23. Cominacini, L.; Pasini, A.F.; Garbin, U.; Davoli, A.; Tosetti, M.L.; Campagnola, M.; Rigoni, A.; Pastorino, A.M.; Cascio, V.L.; Sawamura, T. Oxidized Low Density Lipoprotein (Ox-Ldl) Binding to Ox-Ldl Receptor-1 in Endothelial Cells Induces the Activation of Nf-Kappab through an Increased Production of Intracellular Reactive Oxygen Species. *J. Biol. Chem.* **2000**, *275*, 12633–12638.
24. Yen, C.H.; Hsieh, C.C.; Chou, S.Y.; Lau, Y.T. 17beta-Estradiol Inhibits Oxidized Low Density Lipoprotein-Induced Generation of Reactive Oxygen Species in Endothelial Cells. *Life Sci.* **2001**, *70*, 403–413.
25. Escargueil-Blanc, I.; Meilhac, O.; Pieraggi, M.-T.; Arnal, J.-F.; Salvayre, R.; Nègre-Salvayre, A. Oxidized LDLs Induce Massive Apoptosis of Cultured Human Endothelial Cells Through a Calcium-Dependent Pathway. *Arter. Thromb. Vasc. Biol.* **1997**, *17*, 331–339. <https://doi.org/10.1161/01.atv.17.2.331>.
26. Poullain, C.; Girard-Valenciennes, E.; Smadja, J. Plants from reunion island: Evaluation of their free radical scavenging and antioxidant activities. *J. Ethnopharmacol.* **2004**, *95*, 19–26. <https://doi.org/10.1016/j.jep.2004.05.023>.
27. Laranjinha, J.A.; Almeida, L.M.; Madeira, V.M. Reactivity of dietary phenolic acids with peroxy radicals: Antioxidant activity upon low density lipoprotein peroxidation. *Biochem. Pharmacol.* **1994**, *48*, 487–494. [https://doi.org/10.1016/0006-2952\(94\)90278-x](https://doi.org/10.1016/0006-2952(94)90278-x).
28. Natella, F.; Nardini, M.; Belelli, F.; Scaccini, C. Coffee drinking induces incorporation of phenolic acids into LDL and increases the resistance of LDL to ex vivo oxidation in humans. *Am. J. Clin. Nutr.* **2007**, *86*, 604–609. <https://doi.org/10.1093/ajcn/86.3.604>.
29. Wu, C.; Luan, H.; Zhang, X.; Wang, S.; Zhang, X.; Sun, X.; Guo, P. Chlorogenic Acid Protects against Atherosclerosis in Apoe^{-/-} Mice and Promotes Cholesterol Efflux from Raw264.7 Macrophages. *PLoS ONE* **2014**, *9*, e95452.
30. Lotito, S.B.; Actis-Goretti, L.; Renart, M.L.; Caligiuri, M.; Rein, D.; Schmitz, H.H.; Steinberg, F.M.; Keen, C.L.; Fraga, C.G. Influence of Oligomer Chain Length on the Antioxidant Activity of Procyanidins. *Biochem. Biophys. Res. Commun.* **2000**, *276*, 945–951. <https://doi.org/10.1006/bbrc.2000.3571>.
31. Hirano, R.; Sasamoto, W.; Matsumoto, A.; Itakura, H.; Igarashi, O.; Kondo, K. Antioxidant Ability of Various Flavonoids against DPPH Radicals and LDL Oxidation. *J. Nutr. Sci. Vitaminol.* **2001**, *47*, 357–362. <https://doi.org/10.3177/jnsv.47.357>.
32. Chen, W.-F.; Deng, S.-L.; Zhou, B.; Yang, L.; Liu, Z.-L. Curcumin and its analogues as potent inhibitors of low density lipoprotein oxidation: H-atom abstraction from the phenolic groups and possible involvement of the 4-hydroxy-3-methoxyphenyl groups. *Free. Radic. Biol. Med.* **2006**, *40*, 526–535. <https://doi.org/10.1016/j.freeradbiomed.2005.09.008>.
33. Ramirez-Tortosa, M.C.; Mesa, M.D.; Aguilera, M.C.; Quiles, J.L.; Baro, L.; Ramirez-Tortosa, C.L.; Martinez-Victoria, E.; Gil, A. Oral administration of a turmeric extract inhibits LDL oxidation and has hypocholesterolemic effects in rabbits with experimental atherosclerosis. *Atherosclerosis* **1999**, *147*, 371–378. [https://doi.org/10.1016/s0021-9150\(99\)00207-5](https://doi.org/10.1016/s0021-9150(99)00207-5).
34. Yang, J.-Y.; Della-Fera, M.A.; Rayalam, S.; Ambati, S.; Hartzell, D.L.; Park, H.J.; Baile, C.A. Enhanced inhibition of adipogenesis and induction of apoptosis in 3T3-L1 adipocytes with combinations of resveratrol and quercetin. *Life Sci.* **2008**, *82*, 1032–1039. <https://doi.org/10.1016/j.lfs.2008.03.003>.
35. Hatia, S.; Septembre-Malaterre, A.; Le Sage, F.; Badiou-Bénéteau, A.; Baret, P.; Payet, B.; D'Hellencourt, C.L.; Gonthier, M.-P. Evaluation of antioxidant properties of major dietary polyphenols and their protective effect on 3T3-L1 preadipocytes and red blood cells exposed to oxidative stress. *Free. Radic. Res.* **2014**, *48*, 387–401. <https://doi.org/10.3109/10715762.2013.879985>.
36. Septembre-Malaterre, A.; Le Sage, F.; Hatia, S.; Catan, A.; Janci, L.; Gonthier, M.P. Curcuma Longa Polyphenols Improve Insulin-Mediated Lipid Accumulation and Attenuate Proinflammatory Response of 3t3-L1 Adipose Cells During Oxidative Stress through Regulation of Key Adipokines and Antioxidant Enzymes. *Biofactors* **2016**, *42*, 418–430.
37. Lou, S.; Wang, Y.; Yu, Z.; Guan, K.; Kan, Q. Curcumin induces apoptosis and inhibits proliferation in infantile hemangioma endothelial cells via downregulation of MCL-1 and HIF-1 α . *Med.* **2018**, *97*, e9562. <https://doi.org/10.1097/md.00000000000009562>.
38. Rice-Evans, C.A.; Miller, N.J.; Bolwell, P.G.; Bramley, P.M.; Pridham, J.B. The Relative Antioxidant Activities of Plant-Derived Polyphenolic Flavonoids. *Free. Radic. Res.* **1995**, *22*, 375–383. <https://doi.org/10.3109/10715769509145649>.
39. Vieira, O.; Escargueil-Blanc, I.; Meilhac, O.; Basile, J.-P.; Laranjinha, J.; Almeida, L.M.; Salvayre, R.; Negre-Salvayre, A. Effect of dietary phenolic compounds on apoptosis of human cultured endothelial cells induced by oxidized LDL. *Br. J. Pharmacol.* **1998**, *123*, 565–573. <https://doi.org/10.1038/sj.bjp.0701624>.
40. Chen, J.-H.; Lee, M.-S.; Wang, C.-P.; Hsu, C.-C.; Lin, H.-H. Autophagic effects of Hibiscus sabdariffa leaf polyphenols and epicatechin gallate (ECG) against oxidized LDL-induced injury of human endothelial cells. *Eur. J. Nutr.* **2017**, *56*, 1963–1981. <https://doi.org/10.1007/s00394-016-1239-4>.
41. Nègre-Salvayre, A.; Fitoussi, G.; Réaud, V.; Pieraggi, M.-T.; Thiers, J.-C.; Salvayre, R. A delayed and sustained rise of cytosolic calcium is elicited by oxidized LDL in cultured bovine aortic endothelial cells. *FEBS Lett.* **1992**, *299*, 60–65. [https://doi.org/10.1016/0014-5793\(92\)80101-1](https://doi.org/10.1016/0014-5793(92)80101-1).
42. Hsiung, G.D.; McTighe, A.H. An animal model for DNA-RNA virus interaction based upon virological and histological findings. *Cancer Res.* **1976**, *36*, 674–677.
43. Meilhac, O.; Escargueil-Blanc, I.; Thiers, J.-C.; Salvayre, R.; Negre-Salvayre, A. Bcl-2 alters the balance between apoptosis and necrosis, but does not prevent cell death induced by oxidized low density lipoproteins. *FASEB J.* **1999**, *13*, 485–494. <https://doi.org/10.1096/fasebj.13.3.485>.
44. Meilhac, O.; Zhou, M.; Santanam, N.; Parthasarathy, S. Lipid peroxides induce expression of catalase in cultured vascular cells. *J. Lipid Res.* **2000**, *41*, 1205–1213.
45. Su, H.; Li, Y.; Hu, D.; Xie, L.; Ke, H.; Zheng, X.; Chen, W. Procyanidin B2 ameliorates free fatty acids-induced hepatic steatosis through regulating TFEB-mediated lysosomal pathway and redox state. *Free. Radic. Biol. Med.* **2018**, *126*, 269–286. <https://doi.org/10.1016/j.freeradbiomed.2018.08.024>.

46. Arcambal, A.; Tailé, J.; Couret, D.; Planesse, C.; Veeren, B.; Diotel, N.; Gauvin-Bialecki, A.; Meilhac, O.; Gonthier, M. Protective Effects of Antioxidant Polyphenols against Hyperglycemia-Mediated Alterations in Cerebral Endothelial Cells and a Mouse Stroke Model. *Mol. Nutr. Food Res.* **2020**, *64*, e1900779. <https://doi.org/10.1002/mnfr.201900779>.
47. Tailé, J.; Arcambal, A.; Clerc, P.; Gauvin-Bialecki, A.; Gonthier, M.-P. Medicinal Plant Polyphenols Attenuate Oxidative Stress and Improve Inflammatory and Vasoactive Markers in Cerebral Endothelial Cells during Hyperglycemic Condition. *Antioxidants* **2020**, *9*, 573. <https://doi.org/10.3390/antiox9070573>.
48. Dobi, A.; Bravo, S.B.; Veeren, B.; Paradelo-Dobarro, B.; Álvarez, E.; Meilhac, O.; Viranaicken, W.; Baret, P.; Devin, A.; Rondeau, P. Advanced glycation end-products disrupt human endothelial cells redox homeostasis: New insights into reactive oxygen species production. *Free. Radic. Res.* **2019**, *53*, 150–169. <https://doi.org/10.1080/10715762.2018.1529866>.
49. Tailé, J.; Patché, J.; Veeren, B.; Gonthier, M.P. Hyperglycemic Condition Causes Pro-Inflammatory and Permeability Alterations Associated with Monocyte Recruitment and Deregulated NfκB/PPARγ Pathways on Cerebral Endothelial Cells: Evidence for Polyphenols Uptake and Protective Effect. *Int. J. Mol. Sci.* **2021**, *22*, 1385.
50. Vinson, J.A. Intracellular Polyphenols: How Little We Know. *J. Agric. Food Chem.* **2019**, *67*, 3865–3870. <https://doi.org/10.1021/acs.jafc.8b07273>.
51. Choi, J.S.; Bae, J.Y.; Kim, D.S.; Li, J.; Kim, J.L.; Lee, Y.J.; Kang, Y.H. Dietary Compound Quercitrin Dampens Vegf Induction and PPARγ Activation in Oxidized Ldl-Exposed Murine Macrophages: Association with Scavenger Receptor Cd36. *J. Agric. Food Chem.* **2010**, *58*, 1333–1341.
52. Nishizuka, T.; Fujita, Y.; Sato, Y.; Nakano, A.; Kakino, A.; Ohshima, S.; Kanda, T.; Yoshimoto, R.; Sawamura, T. Procyanidins are potent inhibitors of LOX-1: A new player in the French Paradox. *Proc. Jpn. Acad. Ser. B* **2011**, *87*, 104–113. <https://doi.org/10.2183/pjab.87.104>.
53. Figueira, I.; Tavares, L.; Jardim, C.; Costa, I.; Terrasso, A.P.; Almeida, A.F.; Govers, C.; Mes, J.J.; Gardner, R.; Becker, J.D.; et al. Blood–brain barrier transport and neuroprotective potential of blackberry-digested polyphenols: An in vitro study. *Eur. J. Nutr.* **2017**, *58*, 113–130. <https://doi.org/10.1007/s00394-017-1576-y>.
54. Chen, M.-L.; Yi, L.; Jin, X.; Xie, Q.; Zhang, T.; Zhou, X.; Chang, H.; Fu, Y.-J.; Zhu, J.-D.; Zhang, Q.-Y.; et al. Absorption of resveratrol by vascular endothelial cells through passive diffusion and an SGLT1-mediated pathway. *J. Nutr. Biochem.* **2013**, *24*, 1823–1829. <https://doi.org/10.1016/j.jnutbio.2013.04.003>.
55. Holvoet, P. Endothelial dysfunction, oxidation of low-density lipoprotein, and cardiovascular disease. *Ther. Apher.* **1999**, *3*, 287–293. <https://doi.org/10.1046/j.1526-0968.1999.00169.x>.
56. Chang, H.-C.; Chen, T.-G.; Tai, Y.-T.; Chen, T.-L.; Chiu, W.-T.; Chen, R.-M. Resveratrol Attenuates Oxidized LDL-Evoked Lox-1 Signaling and Consequently Protects against Apoptotic Insults to Cerebrovascular Endothelial Cells. *Br. J. Pharmacol.* **2010**, *31*, 842–854. <https://doi.org/10.1038/jcbfm.2010.180>.
57. Liu, Y.; Chen, X.; Li, J. Resveratrol protects against oxidized low-density lipoprotein-induced human umbilical vein endothelial cell apoptosis via inhibition of mitochondrial-derived oxidative stress. *Mol. Med. Rep.* **2017**, *15*, 2457–2464. <https://doi.org/10.3892/mmr.2017.6304>.
58. Ou, H.-C.; Chou, F.-P.; Sheen, H.-M.; Lin, T.-M.; Yang, C.-H.; Sheu, W.H.-H. Resveratrol, a polyphenolic compound in red wine, protects against oxidized LDL-induced cytotoxicity in endothelial cells. *Clin. Chim. Acta* **2006**, *364*, 196–204. <https://doi.org/10.1016/j.cccn.2005.06.018>.
59. Ou, H.-C.; Lee, W.-J.; Lee, S.-D.; Huang, C.-Y.; Chiu, T.-H.; Tsai, K.-L.; Hsu, W.-C.; Sheu, W.H.-H. Ellagic acid protects endothelial cells from oxidized low-density lipoprotein-induced apoptosis by modulating the PI3K/Akt/eNOS pathway. *Toxicol. Appl. Pharmacol.* **2010**, *248*, 134–143. <https://doi.org/10.1016/j.taap.2010.07.025>.
60. Li, P.; Zhang, L.; Zhou, C.; Lin, N.; Liu, A. Sirt 1 activator inhibits the AGE-induced apoptosis and p53 acetylation in human vascular endothelial cells. *J. Toxicol. Sci.* **2015**, *40*, 615–624. <https://doi.org/10.2131/jts.40.615>.